

Search for Heavy Neutral Leptons with IceCube DeepCore

Dissertation

zur Erlangung des akademischen Grades
doctor rerum naturalium
(Dr. rer. nat.)

im Fach: Physik
Spezialisierung: Experimentalphysik

eingereicht an der
Mathematisch-Naturwissenschaftlichen Fakultät
der Humboldt-Universität zu Berlin

von

Leander Fischer M. Sc.
geboren am 24. Oktober 1992
in Heidelberg

Präsidentin der Humboldt-Universität zu Berlin
Prof. Dr. Julia von Blumenthal

Dekanin der Mathematisch-Naturwissenschaftlichen Fakultät
Prof. Dr. Caren Tischendorf

Copyright Notice

This book is released into the public domain using the CC-BY-4.0 code.

To view a copy of the CC-BY-4.0 code, visit:

<https://creativecommons.org/licenses/by/4.0/>

Colophon

This document was typeset with the help of KOMA-Script and L^AT_EX using the open-source kaobook template class.

The source code of this thesis is available at:

https://github.com/LeanderFischer/phd_thesis

Todo list

add fancy icecube picture	1
exchange for figure with scattering (check abs/sca is cocorrect)	2
mention/cite dust logger paper/procedure?	2
Throw this in a box	3
Add reference for these processes.	6
cite em shower distribution	6
add angular profile plot? (create one based on leif Radel as alex did)	6
cite selection/filtering section	8
increase main text width (read in kao docu)	9
add short description of the processing levels (up to L5?)	11
add short description of the reconstruction (L6 to final?)	11
write bullet points into full sentences for event generation section (read another thesis for more info) .	11
add captions of the cylinder volume table	12
put a number on this significant increase?	13
which experiments measure the axial mass?	15
add varied total cross-section for a few background HNL events	15
add final level effects of varying the axial mass parameters (or example of one)	15
add DIS systematic effect on final level histograms	15
add muon systematic effects (total scale and) on final level histograms	16

Contents

Contents	v
1 The IceCube Neutrino Observatory	1
1.1 Detector Components	1
1.1.1 Digital Optical Modules and the Antarctic Ice	2
1.1.2 IceCube	3
1.1.3 DeepCore	3
1.2 Particles Propagation in Ice	4
1.2.1 Cherenkov Effect	4
1.2.2 Energy Losses	5
1.3 Event Morphologies	7
2 Standard Model Background Simulation and Data Processing	11
2.1 Event Generation	11
2.1.1 Neutrinos	12
2.1.2 Muons	13
2.2 Detector Simulation	13
2.2.1 Photon Propagation	13
2.2.2 Detector Responses	13
2.3 Processing	14
2.3.1 Trigger and Online Filter	14
2.3.2 Offline Filter	14
2.3.3 Hit Selection	14
2.4 Reconstruction	14
2.5 Systematic Uncertainties	15
2.5.1 Atmospheric Flux	16
2.5.2 Detector Property Variations	16
Bibliography	17

List of Figures

1.1	IceCube overview	1
1.2	IceCube sideview	2
1.3	Digital Optical Module (DOM)	3
1.4	IceCube top view	4
1.5	Cherenkov light front	5

List of Tables

1.1	IceCube event signatures and underlying interactions	8
2.1	xx	12

The IceCube Neutrino Observatory

1

The IceCube Neutrino Observatory [1] is a cubic-kilometer, ice-Cherenkov detector located at the geographic South Pole. IceCube utilizes the Antarctic glacial ice as detector medium to observe neutrinos by measuring the Cherenkov light produced from secondary charged particles with optical modules. It was deployed between 2006 and 2011 and has been taking data since the installation of the first modules. The primary goal of IceCube is the observation of astrophysical neutrinos as a telescope, but it can also be used to study fundamental particle physics properties by measuring atmospheric neutrinos as well as studying cosmic rays.

This chapter first describes the main- and sub-array of the detector and its detection module in Section 1.1, the propagation of particles through ice is explained in Section 1.2, and finally, the signatures that IceCube can observe of the different particles are introduced in Section 1.3.

add fancy icecube picture

1.1	Detector Components . . .	1
1.2	Particles Propagation in Ice	4
1.3	Event Morphologies	7

[1]: Aartsen et al. (2017), “The IceCube Neutrino Observatory: instrumentation and online systems”

1.1 Detector Components

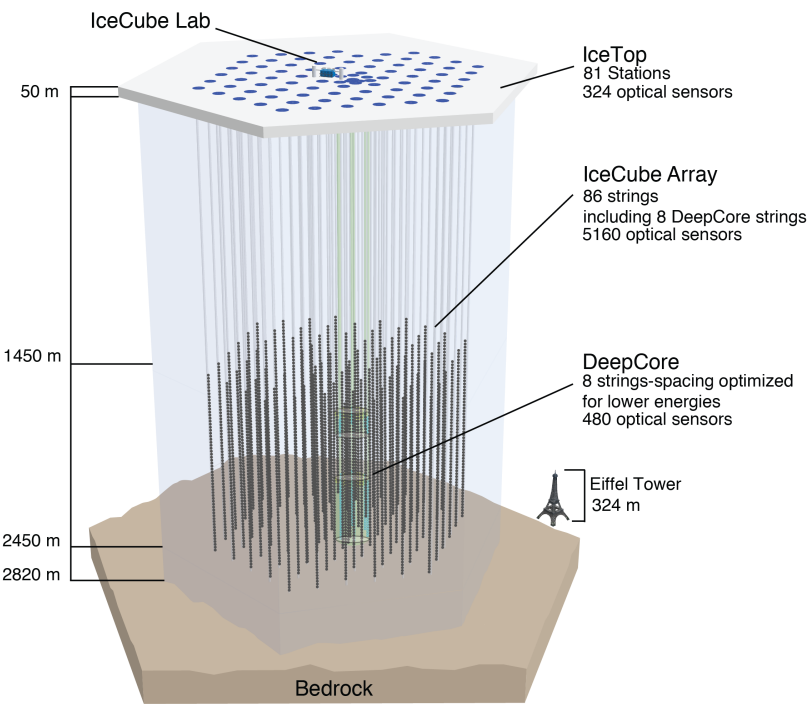


Figure 1.1: Overview of the IceCube detector showing the in-ice main- and sub-array IceCube and DeepCore, IceTop, and the IceCube Lab. From [1].

The full IceCube detector array consists of 86 vertical, in-ice strings and 81 surface stations as shown in Figure 1.1. The in-ice part is composed of 60 optical modules per string deployed at depths of 1450 m–2450 m below the ice, while the surface stations of the comic air-shower array, *IceTop*, are ice-filled tanks. The surface stations and the majority of the strings are arranged in a hexagonal grid with the operations building, the *IceCube Laboratory* (ICL), central to the grid on the surface. A top view

of the hexagonal arrangement is shown in Figure 1.4. The in-ice array is designed to detect neutrinos in the energy range from GeV to PeV.

1.1.1 Digital Optical Modules and the Antarctic Ice

The IceCube detection medium is the Antarctic glacial ice itself, which was formed over 100 000 years by accumulation of snow that was subsequently compressed by its own weight to form a dense crystal structure [2]. As a result of this formation process, the optical properties, scattering and absorption, primarily change with depth. Within the detector volume the absorption length ranges from 100 m–400 m, while the scattering length lies between 20 m and 100 m. They are correlated, with the absorption length being roughly four times the scattering length [3]. The vertical distribution of scattering and absorption length can be seen in Figure 1.2, where one dominant feature is the *dust layer* between 2000 m and 2100 m depth. This region has a higher concentration of dust particles that were deposited in a period of high volcanic activity, which leads to bad optical properties in form of larger scattering and absorption.

[2]: Price et al. (2000), “Age vs depth of glacial ice at South Pole”

[3]: Abbasi et al. (2022), “In-situ estimation of ice crystal properties at the South Pole using LED calibration data from the IceCube Neutrino Observatory”

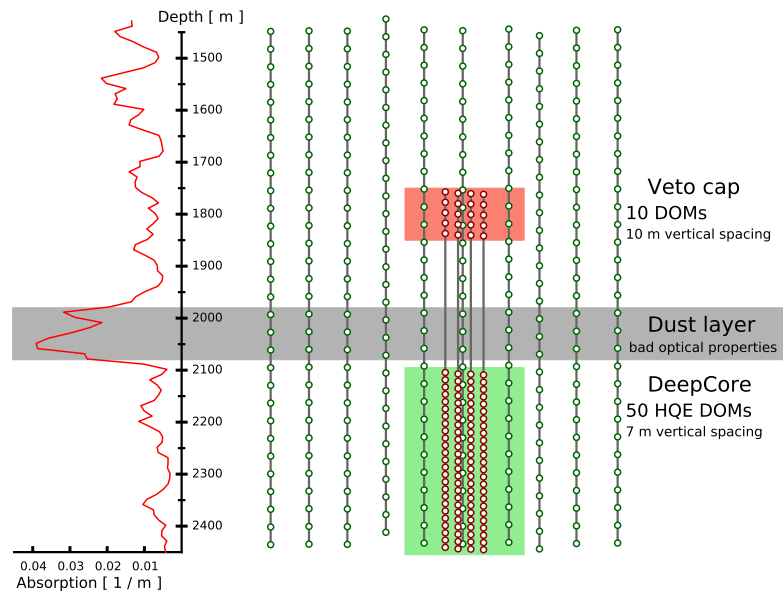


Figure 1.2: Side view of IceCube and DeepCore showing the depth dependent scattering and absorption length (left panel) and the DOM positions around the dust layer.

exchange for figure with scattering (check abs/sca is correct)

mention/cite dust logger paper/procedure?

[4]: Abbasi et al. (2009), “The IceCube data acquisition system: Signal capture, digitization, and timestamping”

[4]: Abbasi et al. (2009), “The IceCube data acquisition system: Signal capture, digitization, and timestamping”

The ice is instrumented by 5160 optical sensors called Digital Optical Modules (DOMs) [4], which can detect the Cherenkov light produced by charged particles traveling through the ice. Each DOM is made of a spherical glass housing, containing a downward-facing Photomultiplier Tube (PMT), the main-board with control, readout, and processing-electronics, and a LED flasher-board for calibration purposes. The design and the individual components of a DOM can be seen in Figure 1.3.

The majority of PMTs are the 10 ” Hamamatsu R7081-02, which have a bialkali photocathode and are sensitive to wavelengths in the range of 300 nm to 650 nm, with a peak quantum efficiency of 25% at 390 nm. In the central part of the IceCube array the peak efficiency reaches 34%. The dark count rate in the temperature range of -40°C to -20°C is ~ 300 Hz. The DOM electronics measure the PMT voltage and control the gain. At a voltage crossing of the equivalent to 0.25 PE the waveform readout is activated [4]. Only when either one of the nearest or next to nearest

DOMs above or below also saw a voltage crossing within a $1\ \mu\text{s}$ time window¹, the voltages are digitized and send to the ICL. Through the application of a waveform unfolding algorithm, called *WaveDeform* [5], the waveforms are compressed and the results are the reconstructed times and charges of the photo-electrons. This is the basis for all further IceCube data processing.

The PMT is covered with a mu-metal grid (made from wire mesh), shielding the photocathode from Earth's magnetic field and it is optically coupled to the glass sphere by RTV silicone gel. The glass sphere is a pressure vessel, designed to withstand both the constant ice pressure and the temporary pressure during the refreezing process of the water in the drill hole during deployment (peaking at around 690 bar). The sphere is held by a harness that connects the DOMs along a string and also guides the cable beside them.

The flasher-board controls 12 LEDs that produce optical pulses in bright UV. The LEDs can be pulsed separately or in combination with variable output levels and pulse lengths. Using the known information of the light source positions and times this can be used for in-situ calibration of the detector by measuring absorption and scattering properties of the ice. Calibrating the optical efficiency of the DOMs itself is more accurately done using minimum ionizing muons [6], since the total amplitude of the LED light is not well known.

1.1.2 IceCube

The 78 strings that are arranged in a hexagonal pattern from the main part of the in-ice array, which is called *IceCube*. With a $\sim 125\ \text{m}$ horizontal spacing between the strings and a $\sim 17\ \text{m}$ vertical spacing between DOMs, IceCube has a lower energy threshold of around 100 GeV. IceCube was designed to detect astrophysical neutrinos with energies above 1 TeV.

The coordinate system that is used in IceCube is centered at 46500'E, 52200'N at an elevation of 883.9 m [1]. Per definition, it's a right-handed coordinate system where the y-axis points along the Prime Meridian (Grid North) towards Greenwich, UK, and the x-axis points 90° clockwise from the y-axis (Grid East). The z-axis is normal to the ice surface, pointing upwards. For IceCube analyses depth is defined as the distance along the z axis from the ice surface, assumed to be at an elevation of 2832 m.

1.1.3 DeepCore

The additional 8 strings form a denser sub-array of IceCube called *DeepCore* [7]. It's located at the bottom-center of the in-ice array and its *fiducial volume* also includes the 7 surrounding IceCube strings as shown in Figure 1.4. The strings in this region have a closer average horizontal distance of about 70 m. The lower 50 DeepCore DOMs on each string are placed in the region of clear ice below the dust layer between 2100 m to 2450 m depth, where their vertical spacing is $\sim 7\ \text{m}$. The remaining 10 modules on each string are placed above the dust layer to be used as veto against atmospheric muons as can be seen in Figure 1.2. Additionally, the

1: This is referred to as a *hard local coincidence (HLC)*.

[5]: Aartsen et al. (2014), "Energy Reconstruction Methods in the IceCube Neutrino Telescope"

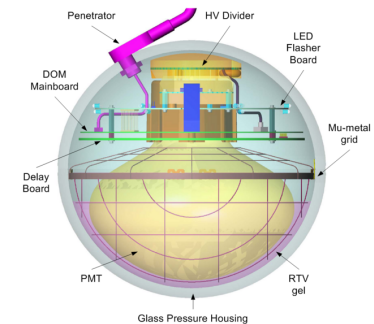


Figure 1.3: Design and components of a Digital Optical Module (DOM) [4]

[6]: Kulacz (2019), "In Situ Measurement of the IceCube DOM Efficiency Factor Using Atmospheric Minimum Ionizing Muons"

[1]: Aartsen et al. (2017), "The IceCube Neutrino Observatory: instrumentation and online systems"

Throw this in a box

[7]: Abbasi et al. (2012), "The design and performance of IceCube DeepCore"

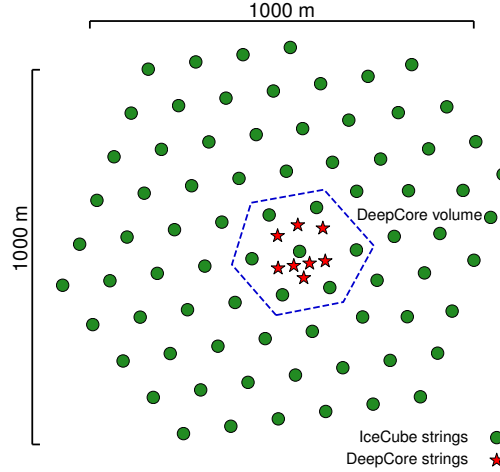


Figure 1.4: Top view of the IceCube array.

DeepCore DOMs are equipped with higher quantum efficiency PMTs. The combination of the denser spacing and the high quantum efficiency modules, leads to a lower energy detection threshold of around 5 GeV, allowing the observation of atmospheric neutrinos, which are mostly in the energy range of 10 GeV to 100 GeV. The main analysis performed with DeepCore is an atmospheric neutrino oscillation measurement, but the large flux of atmospheric neutrinos allows for many other Beyond Standard Model searches, such as searches for dark matter, non-standard interactions, or sterile neutrinos.

1.2 Particles Propagation in Ice

Neutrinos interacting in the ice via DIS produce muons, electromagnetic showers, and hadronic showers, depending on their flavor and the interaction type. The particles produced in those processes mainly lose their energy through *ionization*, *bremsstrahlung*, *pair production*, and the *photo-nuclear interaction*. Electrically charged particles also emit Cherenkov light when traveling through the ice, which is the main observable in IceCube, but only contributes a small amount to the total energy loss. The Cherenkov effect and the energy losses of the particles are described in the following sections, followed by an overview of the different particle signatures in IceCube.

1.2.1 Cherenkov Effect

When a charged particle moves through a medium with a velocity that is greater than the speed of light in that medium, it emits Cherenkov radiation, losing a very small amount of energy ($\mathcal{O}(10^{-4})$ of the total energy loss). The detection principle of IceCube and DeepCore however, is based fundamentally on the observation of resulting Cherenkov photons that are emitted by the charged secondary particles produced in the neutrino interactions that were introduced in Section ???. The Cherenkov effect was first observed by Pavel Cherenkov in 1934 [8] and occurs when the charged particle travels faster than the phase velocity of light, therefore polarizing the medium. Upon de-excitation the molecules emit the received energy

[8]: Cherenkov (1937), “Visible Radiation Produced by Electrons Moving in a Medium with Velocities Exceeding that of Light”

as photons in a spherical wavefront. Since the particle moves past this wavefront, the superposition of the spherical light emissions form a cone which is shown in blue in the bottom of Figure 1.5.

Using trigonometry, the angle θ_c at which the Cherenkov light is emitted can be calculated as

$$\theta_c = \arccos\left(\frac{1}{\beta n}\right), \quad (1.1)$$

where β is the velocity of the particle in units of the speed of light and n is the refractive index of the medium. When the particle velocity is close to the speed of light, the equation holds and the angle is only dependent on the refractive index of the medium. For the Antarctic ice, the refractive index is $n \approx 1.3$ and as a result $\theta_c \approx 41^\circ$ [9].

The frequency of the emission depends on the charge z and the wavelength-dependent index of refraction $n(\omega)$ and is given by the Frank-Tamm formula [10, 11]

$$\frac{d^2N}{dx d\lambda} = \frac{2\pi\alpha z^2}{\lambda^2} \left(1 - \frac{1}{\beta^2 n(\omega)^2}\right), \quad (1.2)$$

with $\alpha \approx 1/137$ the fine structure constant, λ the wavelength of the emitted light, and x the path length traversed by the particle. Relativistic particles in ice produce roughly 250 photons per cm in the wavelength range of 300 nm-500 nm [12].

1.2.2 Energy Losses

Even though relativistic, charged particles traveling through matter produce Cherenkov radiation, their energy is mainly lost through other processes that are dependent on the particle type and energy. The exact principles of energy loss for the different types can broadly be categorized into the three groups: quasi-continuous energy loss by muons, electromagnetic cascades, and hadronic cascades.

Muons

Muons lose their energy by ionization, bremsstrahlung, pair production, and the photo-nuclear effect. The energy loss by ionization is the dominant process for muons above 1 GeV and has a weak energy dependence given by

$$\left\langle -\frac{dE}{dx} \right\rangle = a_I(E) + b_R(E) \cdot E, \quad (1.3)$$

where E is the energy and $a_I(E)$ and $b_R(E) \cdot E$ are the energy loss by ionization and the combined radiative losses, respectively. In the energy range relevant for this work (10 GeV-100 GeV), the parameters a_I and b_R only depend on energy very weakly and can be approximated by constants. The energy loss is then given by

$$\left\langle -\frac{dE}{dx} \right\rangle = a + b \cdot E. \quad (1.4)$$

Based on this description, there is a critical energy which divides the regimes where ionization and radiative losses dominate. The critical

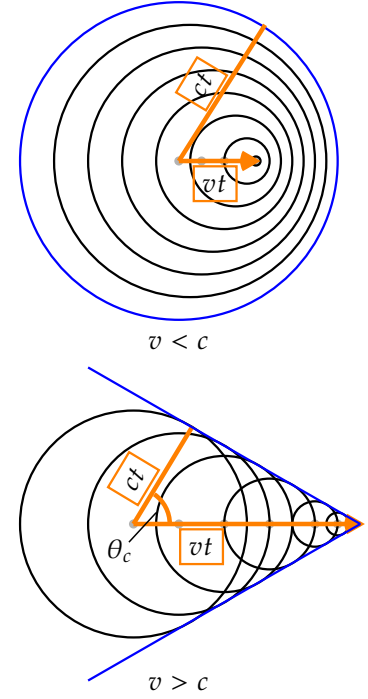


Figure 1.5: Schematic depiction of the spherical light front produced by a particle traveling slower than the speed of light in the medium (top) and the formation of the Cherenkov light front produced by a charged particle traveling faster than the speed of light in the medium (bottom). Blue is the resulting wavefront, while the black circles are spherically emitted light at each position and the orange arrows show the direction of the particle.

[9]: Euler (2014), "Observation of oscillations of atmospheric neutrinos with the IceCube Neutrino Observatory"

[10]: Frank et al. (1937), "Coherent visible radiation from fast electrons passing through matter"

[11]: Tamm (1991), "Radiation Emitted by Uniformly Moving Electrons"

[12]: Radel et al. (2012), "Calculation of the Cherenkov light yield from low energetic secondary particles accompanying high-energy muons in ice and water with Geant4 simulations"

[13]: Chirkin et al. (2004), “Propagating leptons through matter with Muon Monte Carlo (MMC)”

energy is given by $E_{crit} = a/b$ and for muons in ice it is ~ 713 GeV (using $a \approx 2.59$ MeV and $b \approx 3.63 \times 10^{-6} \text{ cm}^{-1}$ [13]). Since the energy range of interest is well below this critical energy the range of a muon can easily related to its energy by

$$\langle L \rangle = \frac{E_0}{a} , \quad (1.5)$$

Measuring the length of a muon track therefore allows for an estimation of its energy if the full track is contained in IceCube. Using the given numbers a 30 GeV muon travels ~ 116 m. This approximate treatment does not take into account the stochastic nature of some energy losses. Bremsstrahlung and photo-nuclear interactions for example occur rarely, but when they do, they deposit a large chunk of energy. A thorough investigation of the energy losses of muons in ice can be found in [14].

[14]: Raedel (2012), “Simulation Studies of the Cherenkov Light Yield from Relativistic Particles in High-Energy Neutrino Telescopes with Geant4”

Electromagnetic Showers

Photons as well as electrons and positrons are produced either directly in neutrino interactions or in secondary particle interactions. Above a critical energy E_c , they lose their energy through pair production and bremsstrahlung, respectively, where the resulting photons and the electron/positron pairs can both produce further particles through repeated pair production and bremsstrahlung emission forming an expanding, electromagnetic shower profile. The particles’ energy reduces with every interaction and their number increases until they fall below the critical energy where ionization and excitation of surrounding atoms become the dominant energy loss processes for electrons and positrons. For photons the remaining energy is lost through the Compton effect and the photoelectric effect. Below the critical energy no new shower particles are produced. Electromagnetic cascades can be characterized by the radiation length, X_0 , after which electrons/positrons reduced their energy to $1/e$ of their initial energy. For photons, it’s equivalent to $7/9$ of the mean free path of pair production. The critical energy for ice is $E_c \approx 78$ MeV, with a radiation length of $X_0 \approx 39.3$ cm [15].

Add reference for these processes.

[15]: Tanabashi et al. (2018), “Review of Particle Physics”

cite em shower distribution

The radiation length governs the longitudinal shower profile and using $t = x/X_0$, the shower intensity can be described by

$$\frac{dE}{dt} = E_0 b \frac{(bt)^{a-1} e^{-bt}}{\Gamma(a)} , \quad (1.6)$$

[14]: Raedel (2012), “Simulation Studies of the Cherenkov Light Yield from Relativistic Particles in High-Energy Neutrino Telescopes with Geant4”

[16]: Agostinelli et al. (2003), “Geant4—a simulation toolkit”

where a and b are parameters that have to be estimated from experiment. Based on the work from [14], performed with Geant4 [16], the parameters for electromagnetic showers in ice are

$$e^- : a \approx 2.01 + 1.45 \log_{10}(E_0/\text{GeV}), b \approx 0.63 , \quad (1.7a)$$

$$e^+ : a \approx 2.00 + 1.46 \log_{10}(E_0/\text{GeV}), b \approx 0.63 , \quad (1.7b)$$

$$\gamma : a \approx 2.84 + 1.34 \log_{10}(E_0/\text{GeV}), b \approx 0.65 . \quad (1.7c)$$

The maximum of the shower is at $t_{max} = (a - 1)/b$ and the Cherenkov emission of the charged particles produced in the shower is peaked around the Cherenkov angle, since they are produced in the forward direction.

add angular profile plot?
(create one based on leif R  del as alex did)

Hadronic Showers

The breaking nucleus or any hadronic decay products from the neutrino DIS interactions always create a hadronic cascade. It is a result of secondary particles produced in strong interactions between the hadrons and the traversed matter. The charged particles produced in the shower will emit Cherenkov radiation, while neutral particles will be invisible to the detector. There is also an electromagnetic component of the shower, due to for example the decay of neutral pions into photons. Hadronic showers of the same energy as electromagnetic showers have larger fluctuations in energy deposition and shape, since they depend on the produced particle types. Hadrons also have a higher energy threshold for Cherenkov light production, because of their higher mass. Based on [14, 17], the visible electromagnetic fraction of hadronic showers can be parameterized as

$$F(E_0) = \frac{T_{\text{hadron}}}{T_{\text{EM}}} = 1 - (1 - f_0) \left(\frac{E_0}{E_s} \right)^{-m}, \quad (1.8)$$

where $T_{\text{hadron/EM}}$ is the total track length of a hadronic/electromagnetic shower with the same energy, f_0 is the ratio of hadronic and electromagnetic light yield, E_0 is the initial energy, and E_s is an energy scale. The parameter m is an arbitrary parameter. The ration $F(E_0)$ increases with energy, but is always smaller than 1. The variance of this distribution is given by

$$\sigma_F(E_0) = \sigma_0 \log(E_0)^{-\gamma}. \quad (1.9)$$

The parameters m , E_s , and f_0 are fit from simulation. Cherenkov light from hadronic showers also peaks around the Cherenkov angle, but the angular distribution is more smeared out, due to the variations in particle type and their energy depositions.

[14]: Raedel (2012), “Simulation Studies of the Cherenkov Light Yield from Relativistic Particles in High-Energy Neutrino Telescopes with Geant4”

[17]: Gabriel et al. (1994), “Energy dependence of hadronic activity”

1.3 Event Morphologies


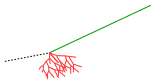

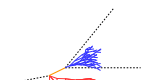
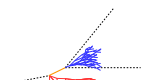

The event morphologies produced by particles detected in IceCube are combinations of the three energy loss types described in Section 1.2.2, e.g. *cascades* from electromagnetic and hadronic showers and elongated *tracks* from muons traveling through the detector. Table 1.1 gives an overview of the possible event signatures.

Neutrino interactions are observed as cascades, tracks, or a combination of both, depending on the initial flavor and the interaction type for the specific event.

In ν_μ - CC interactions, a muon is produced in addition to a hadronic shower from the breaking nucleus. If the interaction happens outside the detector, but the muon passes through the detector, this will create a track-like signature. Same happens if the interaction happens inside, but the energy transfer to the nucleus is small ($y \approx 0$). At energies relevant for this work, tracks have length at the same order of the distance between DOMs, so they can be observed as such.

If the interaction happens inside the detector and the energy transfer to the hadronic part of the shower is larger, it will create a cascade with

Table 1.1: IceCube event signatures, their underlying interaction type, and the particles that produce them. Also shown are the secondary particles produced in the interactions. Black dashed lines represent neutrinos, green lines muons, orange line leptons, and blue and red lines are particles in electromagnetic and hadronic cascades, respectively. Adapted from [18].

Interaction	Secondary particles	Signature
$\text{CC } \nu_\mu^{(-)}$	 μ^\pm track	Track-only
	 μ^\pm track and hadrons	Track with cascade
$\text{CC } \nu_\tau^{(-)}$	 τ^\pm decaying into μ^\pm ($\sim 17\%$ BR), hadrons	Cascade with track
	 τ^\pm decaying into e^\pm or hadrons ($\sim 83\%$ BR)	
$\text{CC } \nu_e^{(-)}$	 e^\pm , hadrons	Cascade-only
$\text{NC } \nu_\ell^{(-)}$	 hadrons	

a track leaving it. A similar signature occurs if a ν_τ - CC interaction happens, creating a tau that decays into a muon (happening with a branching ratio of 17%). In those cases the muon usually has a lower energy and the track will be fainter and harder to observe.

The other 83 % of ν_τ - CC interactions produce a tau that decays into an electron or hadrons, leaving a cascade-only signature through the electromagnetic or hadronic shower. All ν_e - CC interactions also produce pure cascades, since the electron quickly loses its energy in an electromagnetic shower. In all ν - NC interactions, the produced neutrino escapes and only the hadronic shower is observable. Since the size of the cascades at the energy range of interest is smaller than the spacing of the DOMs, they are approximately observed as point-like, spherical light sources. Considering the short effective scattering length (20 m-50 m), the light is almost isotopically emitted.

Atmospheric muons also produce pure track like signatures, similar to ν_μ - CC interactions happening outside the detector. They are one of the main backgrounds for analyses using atmospheric neutrinos and are therefore the target of many filter steps described in.

cite selection/filtering section

increase main text width
(read in kao docu)

Standard Model Background Simulation and Data Processing

2

The analysis presented in this thesis is highly dependent on an efficient event selection to reduce the raw IceCube trigger data to a usable atmospheric neutrino sample and on a precise estimation of both expected SM background and BSM signal events through MC simulations. This chapter describes the current simulation and event selection chain used for state-of-the-art IceCube neutrino oscillation measurements like [19]. The whole chain can be broadly split into 4 steps:

Step 1 Event Generation: The initial step for all particle (non-noise) simulation is the generation of events using chosen initial distributions and fluxes. Events are usually the primary particle and the particles produced in the interaction with the ice.

Step 2 Detector Simulation: The particles from the first step are propagated through the ice, producing Cherenkov photons, which are then propagated further. If they hit a DOM the full detector response (PMT, readout, trigger and online processing) is simulated.

Step 3 Processing:

Step 4 Reconstruction:

This chapter only describes the event generation for the SM background simulation (neutrinos and muons), while the signal simulation is described in Chapter ???. The detector simulation is identical for both signal and background events while processing and reconstruction are applied to all simulation and data in the same way. Splitting the simulation steps has the advantage of reusing the outputs of for example the generation step to propagate the particles with different ice model, in order to estimate the systematic impacts of uncertainties of the ice properties. Similar approach can be taken for varying detector response and through this a more efficient (reduced) use of computing resources can be achieved. The following sections describe the different steps in more detail and the last section, Section 2.5, describes the related systematic uncertainties considered for this work.

2.1	Event Generation	11
2.2	Detector Simulation	13
2.3	Processing	14
2.4	Reconstruction	14
2.5	Systematic Uncertainties .	15

[19]: Abbasi et al. (2023), “Measurement of atmospheric neutrino mixing with improved IceCube DeepCore calibration and data processing”

add short description of the processing levels (up to L5?)

add short description of the reconstruction (L6 to final?)

2.1 Event Generation

The MC is used in the analysis by applying a method called *forward folding*, where a very large number of events (signal and background) is produced using sampling distribution that are tuned to have a large selection efficiency. Those distributions don’t have to be physically correct distributions, but they need to cover the full parameter space of interest for the analysis. To produce the correct physical distributions each event gets a weight, which can be used to estimate the expected number of events given a specific choice of physics and nuisance parameters. The large number of raw MC events ensures a good estimation of the expected numbers and weighted distributions.

The analysis itself is then performed by comparing the weighted MC distributions to the observed data. This is done by binning them as will

write bullet points into full sentences for event generation section (read another thesis for more info)

be described in Chapter ?? and calculating a loss function comparing the bin expectations to the data. By varying the physics and nuisance parameters, that govern the weights, the loss function can be minimized and the parameters producing MC that describes the data best are found. In order to achieve a reliable result with this method the MC needs to be precise and as close to the data as possible (at least at the final selection step).

2.1.1 Neutrinos

Due to the very low interaction rate of neutrinos, the event generation is performed in a way that forces every event to interact in a chosen sampling volume. The weight of each event is then calculated as the inverse of the simulated neutrino fluence

$$w = \frac{1}{F_{\text{sim}}} \frac{1}{N_{\text{sim}}} , \quad (2.1)$$

where F_{sim} is the number of neutrino events per energy, time, area, and solid angle and N_{sim} is the number of simulated events. If this weight is multiplied by the livetime and the theoretically expected neutrino flux for a given physical model, it results in the number of events that this event would produce. The used baseline neutrino flux computed for the South Pole is taken from [20].

[20]: Honda et al. (2015), “Atmospheric neutrino flux calculation using the NRLMSISE-00 atmospheric model”

The chosen simulation volume is a cylinder centered in DeepCore with radius and height chosen such that all events possibly producing a signal are contained. The different sizes are chosen depending on energy and neutrino flavor are shown in Table 2.1. The directions of the neutrinos

Table 2.1: xx

Flavor	Energy [GeV]	Radius [m]	Length [m]	Events/File	Files
$\nu_e + \bar{\nu}_e$	1-4	250	500	450000	650
	4-12			100000	
	12-100	350	600	57500	
	100-10000	550	1000	57500	
$\nu_\mu + \bar{\nu}_\mu$	1-5	250	500	408000	1550
	5-80	400	900	440000	
	80-1000	450	1500	57500	
	1000-10000	550		6700	
$\nu_\tau + \bar{\nu}_\tau$	1-4	250	500	1500000	350
	4-10			300000	
	10-50	350	600	375000	
	50-1000	450	800	200000	
	1000-10000	550	1500	26000	

add captions of the cylinder volume table

are sampled isotropically in zenith and azimuth and the energies are sampled from a power law E^{-2} . The number of simulated events is chosen such that the livetime is more than 70 years for each flavor. Neutrinos and antineutrinos are simulated with ratios of 70% and 30%, respectively.

To simulate the neutrino interaction with the ice the GENIE event generator [21] is used resulting in the secondary particles and the kinematic and cross-section parameters. Muons produced in these interactions are propagated using PROPOSAL [22], also simulating their Cherenkov light output. The shower development of gamma rays, electrons, and positrons below 100 MeV and hadronic showers below 30 GeV is simulated using GEANT4 [16] while for higher energies an analytical approximation from [12] is used.

2.1.2 Muons

Atmospheric muons are generated on a cylinder surface enclosing the full IceCube detector array. The cylinder has a height of 1600 m and a radius of 800 m. The energy is sampled from an E^{-3} power law while the other sampling distributions (position, direction) are found from parameterizations based on [23]. This work uses full CORSIKA [24] simulations of muons to tailor the parameterizations, starting from cosmic ray interactions with atmospheric nuclei using the cosmic ray flux model from [25] and producing the muons applying the hadronic interaction model SIBYLL 2.1 [26]. After the generation, they are propagated through the ice with PROPOSAL producing photons, treating them exactly like the muons produced in neutrino interactions.

Since the offline processing and selection steps described in Section 2.3.2 and Section 2.4 reduce the muon contamination to a negligible level, it is difficult to correctly estimate the expected number of muon events at final selection level and therefore two separate sets of muon simulation are produced. A **first set** including all events resulting from the above described generation to tune the lower level selection (up to L4) and a **second set** to estimate the muon contamination at higher levels (above L5), which only accepts muon events if they pass through a smaller cylinder centered in DeepCore (height of 400 m and radius of 180 m) and rejects events based on a KDE estimated muon density at L5 (in energy and zenith) increasing the simulation efficiency at L5 significantly .

[21]: Andreopoulos et al. (2015), “The GENIE Neutrino Monte Carlo Generator: Physics and User Manual”

[22]: Koehne et al. (2013), “PROPOSAL: A tool for propagation of charged leptons”

[16]: Agostinelli et al. (2003), “Geant4—a simulation toolkit”

[12]: Rädcl et al. (2012), “Calculation of the Cherenkov light yield from low energetic secondary particles accompanying high-energy muons in ice and water with Geant4 simulations”

[23]: Becherini et al. (2006), “A parameterisation of single and multiple muons in the deep water or ice”

[24]: Heck et al. (1998), “CORSIKA: A Monte Carlo code to simulate extensive air showers”

[25]: Gaisser (2012), “Spectrum of cosmic-ray nucleons, kaon production, and the atmospheric muon charge ratio”

[26]: Engel et al. (2017), “The hadronic interaction model Sibyll – past, present and future”

put a number on this significant increase?

2.2 Detector Simulation

2.2.1 Photon Propagation

- CLSIM [27] which is an implementation of PPC[28] in OPENCL -

[27]: Kopper et al. (),

[28]: Chirkin et al. (2019), “Photon Propagation using GPUs by the IceCube Neutrino Observatory”

2.2.2 Detector Responses

- Monte Carlo photo-electron (MCPE) - single photo-electron (SPE) -

2.3 Processing

2.3.1 Trigger and Online Filter

2.3.2 Offline Filter

2.3.3 Hit Selection

[29]: Garza (2014), “Measurement of neutrino oscillations in atmospheric neutrinos with the IceCube DeepCore detector”

To select hits that originated from direct photons, a procedure closely related to the one described in [29] is applied. The cleaning is based on removing hits from DOMs that could have originated from light emitted by any of the other hit DOMs on the same string. The selection solely uses the time of arrival (TOA) of the pulses. It is carried out for every detected event in the following steps:

2.4 Reconstruction

[30]: Lundberg et al. (2007), “Light tracking for glaciers and oceans: Scattering and absorption in heterogeneous media with Photonics”

There are several methods to select and reconstruct events in IceCube. At energies around 10-40 GeV, where we expect the oscillation signal, the events are faint and only a few DOMs detect light. One approach for the reconstruction of such events is described in this section. The reconstruction uses only photons that traveled along a straight line - called *direct* photons. Using direct photons has the benefit of reducing the systematic biases caused by the large variations of the bulk ice properties; scattering and absorption. With an average distance of 70 m between strings in DeepCore and an effective scattering length of about 50 m [30], there will always be a fraction of direct photons arriving at the DOMs. The used method applies a stepwise procedure, where first a cleaning routine selects events with direct photons as described in Section 2.3.3. Afterward, the direction of the particle is reconstructed and finally the energy is determined as outlined in Section 2.4.

FLERCNN Event Reconstruction and Classification

Didn't copy over SANTA/LEERA since I need the FLERCNN description here.

Standard Model Event Morphologies

The signals that IceCube detects vary depending on the neutrino flavor and interaction type of the event. The two main signatures that can be observed are track-like and cascade-like events. The observed Cherenkov light is produced by the secondary particles originating from the neutrino interactions described in Section ???. Table 1.1 shows an overview of the possible event signatures. Minimum ionizing muons can travel for long distances and are seen as extended light signatures called tracks. Muons can come from ν_μ -CC interactions or from ν_τ -CC followed by the decay of the τ to a muon. However, the τ only decays to a muon with a branching ratio of BR=17 %.

Cascades are the light signal produced by the EM/hadronic showers described in Section 1.2.2. They come from ν_e -CC and most of the ν_τ -CC interactions because the electron and the tau lose all their energy quickly and only travel a short distance. They are also produced in all ν -NC interactions since only the hadronic shower is observable and the produced neutrino escapes unseen. The cascades at the energies considered in this work have a smaller radius than the spacing of the DOMs and are therefore seen as point-like light emitters.

The existence of the two types of event morphologies and their origins imply that by identifying track-like events we can identify events coming (mainly) from ν_μ -CC interactions and therefore obtain a flavor identification. This is a crucial part of performing an oscillation analysis as will be further discussed in Section ??.

Final Level Event Selection

add this here or in the analysis chapters?

2.5 Systematic Uncertainties

Neutrino Cross-Section Systematic Uncertainties

- three cross-section uncertainties are included, two for uncertainties in form factors of charged-current quasi-elastic (CCQE) and charged-current resonance (CCRES) events and for uncertainties in deep inelastic scattering (DIS) events
- the uncertainties in the form factors are due to uncertainties in the *axial mass* M_A which enters the form factor as in

$$F(Q^2) \sim \frac{1}{(1 - (\frac{Q}{M_A})^2)^2}, \quad (2.2)$$

where Q^2 is the momentum transfer squared

which experiments measure the axial mass?

- the axial mass can be determined experimentally and to include uncertainties on the values of M_A^{CCQE} and M_A^{CCRES} , the cross-sections are computed with GENIE where the form factors are calculated varying the axial mass by $\pm 20\%(1\sigma)/\pm 40\%(1\sigma)$ around the nominal value - this is an approximation of the recommended uncertainties by the GENIE collaboration, which are -15% , $+25\%$ for M_A^{CCQE} and $\pm 20\%$ for M_A^{CCRES} [21] - to apply a continuous uncertainty variation of the axial mass in a fit, the total cross-section is fit with a quadratic function to interpolate between the cross-sections computed with the different axial masses

add varied total cross-section for a few background HNL events

add final level effects of varying the axial mass parameters (or example of one)

- the uncertainty parameter of the DIS cross-section is based on the discrepancy between the cross-sections computed with GENIE and the ones computed with CSMS [31] above 100 GeV - the included parameter scales the cross-section from the GENIE values to the CSMS values, which are considered more accurate above 100 GeV - below 100 GeV the scaling is extrapolated linearly

[31]: Cooper-Sarkar et al. (2011), "The high energy neutrino cross-section in the Standard Model and its uncertainty"

add DIS systematic effect on final level histograms

2.5.1 Atmospheric Flux

2.5.2 Detector Property Variations

Muon Uncertainties

- final level muon fraction is below a percent - just include a total scaling parameter in the analysis (- total scale is degenerate with DOM efficiency, since increased DOM efficiency approximately leads to better muon rejection) - changes in the muon spectral index have a negligible effect on the final level histograms and the analysis (see systematic impact test in section xx)

add muon systematic effects
(total scale and) on final
level histograms

Bibliography

Here are the references in citation order.

- [1] M. G. Aartsen et al. “The IceCube Neutrino Observatory: instrumentation and online systems”. In: *Journal of Instrumentation* 12.3 (Mar. 2017), P03012. doi: [10.1088/1748-0221/12/03/P03012](https://doi.org/10.1088/1748-0221/12/03/P03012) (cited on pages 1, 3).
- [2] P. B. Price, K. Woschnagg, and D. Chirkin. “Age vs depth of glacial ice at South Pole”. In: *Geophysical Research Letters* 27.14 (2000), pp. 2129–2132. doi: <https://doi.org/10.1029/2000GL011351> (cited on page 2).
- [3] R. Abbasi et al. “In-situ estimation of ice crystal properties at the South Pole using LED calibration data from the IceCube Neutrino Observatory”. In: *The Cryosphere Discussions* 2022 (2022), pp. 1–48. doi: [10.5194/tc-2022-174](https://doi.org/10.5194/tc-2022-174) (cited on page 2).
- [4] R. Abbasi et al. “The IceCube data acquisition system: Signal capture, digitization, and timestamping”. In: *Nuclear Instruments and Methods in Physics Research Section A: Accelerators, Spectrometers, Detectors and Associated Equipment* 601.3 (2009), pp. 294–316. doi: <https://doi.org/10.1016/j.nima.2009.01.001> (cited on pages 2, 3).
- [5] M. G. Aartsen et al. “Energy Reconstruction Methods in the IceCube Neutrino Telescope”. In: *JINST* 9 (2014), P03009. doi: [10.1088/1748-0221/9/03/P03009](https://doi.org/10.1088/1748-0221/9/03/P03009) (cited on page 3).
- [6] N. Kulacz. “In Situ Measurement of the IceCube DOM Efficiency Factor Using Atmospheric Minimum Ionizing Muons”. MA thesis. University of Alberta, 2019 (cited on page 3).
- [7] R. Abbasi et al. “The design and performance of IceCube DeepCore”. In: *Astropart. Phys.* 35.10 (2012), pp. 615–624. doi: [10.1016/j.astropartphys.2012.01.004](https://doi.org/10.1016/j.astropartphys.2012.01.004) (cited on page 3).
- [8] P. A. Cherenkov. “Visible Radiation Produced by Electrons Moving in a Medium with Velocities Exceeding that of Light”. In: *Phys. Rev.* 52 (4 Aug. 1937), pp. 378–379. doi: [10.1103/PhysRev.52.378](https://doi.org/10.1103/PhysRev.52.378) (cited on page 4).
- [9] S. Euler. “Observation of oscillations of atmospheric neutrinos with the IceCube Neutrino Observatory”. PhD thesis. Aachen, Germany: Rheinisch-Westfälischen Technischen Hochschule, 2014 (cited on page 5).
- [10] I. Frank and I. Tamm. “Coherent visible radiation from fast electrons passing through matter”. In: *C. R. Acad. Sci. USSR* 14 (1937), pp. 109–114 (cited on page 5).
- [11] I. Tamm. “Radiation Emitted by Uniformly Moving Electrons”. In: *Selected Papers*. Ed. by B. M. Bolotovskii, V. Y. Frenkel, and R. Peierls. Berlin, Heidelberg: Springer Berlin Heidelberg, 1991, pp. 37–53. doi: [10.1007/978-3-642-74626-0_3](https://doi.org/10.1007/978-3-642-74626-0_3) (cited on page 5).
- [12] L. Rädcl and C. Wiebusch. “Calculation of the Cherenkov light yield from low energetic secondary particles accompanying high-energy muons in ice and water with Geant4 simulations”. In: *Astroparticle Physics* 38 (Oct. 2012), pp. 53–67. doi: [10.1016/j.astropartphys.2012.09.008](https://doi.org/10.1016/j.astropartphys.2012.09.008) (cited on pages 5, 13).
- [13] D. Chirkin and W. Rhode. “Propagating leptons through matter with Muon Monte Carlo (MMC)”. In: (July 2004) (cited on page 6).
- [14] L. Raedel. “Simulation Studies of the Cherenkov Light Yield from Relativistic Particles in High-Energy Neutrino Telescopes with Geant4”. MA thesis. Aachen, Germany: Rheinisch-Westfälischen Technischen Hochschule, 2012 (cited on pages 6, 7).
- [15] M. Tanabashi et al. “Review of Particle Physics”. In: *Phys. Rev. D* 98 (3 Aug. 2018), p. 030001. doi: [10.1103/PhysRevD.98.030001](https://doi.org/10.1103/PhysRevD.98.030001) (cited on page 6).
- [16] S. Agostinelli et al. “Geant4—a simulation toolkit”. In: *Nucl. Instr. Meth. Phys. Res.* 506.3 (July 2003), pp. 250–303. doi: [10.1016/S0168-9002\(03\)01368-8](https://doi.org/10.1016/S0168-9002(03)01368-8) (cited on pages 6, 13).

- [17] T. Gabriel et al. “Energy dependence of hadronic activity”. In: *Nuclear Instruments and Methods in Physics Research Section A: Accelerators, Spectrometers, Detectors and Associated Equipment* 338.2 (1994), pp. 336–347. doi: [https://doi.org/10.1016/0168-9002\(94\)91317-X](https://doi.org/10.1016/0168-9002(94)91317-X) (cited on page 7).
- [18] A. Terliuk. “Measurement of atmospheric neutrino oscillations and search for sterile neutrino mixing with IceCube DeepCore”. PhD thesis. Berlin, Germany: Humboldt-Universität zu Berlin, Mathematisch-Naturwissenschaftliche Fakultät, 2018. doi: [10.18452/19304](https://doi.org/10.18452/19304) (cited on page 8).
- [19] R. Abbasi et al. “Measurement of atmospheric neutrino mixing with improved IceCube DeepCore calibration and data processing”. In: *Phys. Rev. D* 108 (1 July 2023), p. 012014. doi: [10.1103/PhysRevD.108.012014](https://doi.org/10.1103/PhysRevD.108.012014) (cited on page 11).
- [20] M. Honda et al. “Atmospheric neutrino flux calculation using the NRLMSISE-00 atmospheric model”. In: *Phys. Rev. D* 92 (2 July 2015), p. 023004. doi: [10.1103/PhysRevD.92.023004](https://doi.org/10.1103/PhysRevD.92.023004) (cited on page 12).
- [21] C. Andreopoulos et al. “The GENIE Neutrino Monte Carlo Generator: Physics and User Manual”. In: (2015) (cited on pages 13, 15).
- [22] J.-H. Koehne et al. “PROPOSAL: A tool for propagation of charged leptons”. In: *Computer Physics Communications* 184.9 (2013), pp. 2070–2090. doi: <https://doi.org/10.1016/j.cpc.2013.04.001> (cited on page 13).
- [23] Y. Becherini et al. “A parameterisation of single and multiple muons in the deep water or ice”. In: *Astroparticle Physics* 25.1 (2006), pp. 1–13. doi: <https://doi.org/10.1016/j.astropartphys.2005.10.005> (cited on page 13).
- [24] D. Heck et al. “CORSIKA: A Monte Carlo code to simulate extensive air showers”. In: (Feb. 1998) (cited on page 13).
- [25] T. K. Gaisser. “Spectrum of cosmic-ray nucleons, kaon production, and the atmospheric muon charge ratio”. In: *Astropart. Phys.* 35 (2012), pp. 801–806. doi: [10.1016/j.astropartphys.2012.02.010](https://doi.org/10.1016/j.astropartphys.2012.02.010) (cited on page 13).
- [26] R. Engel et al. “The hadronic interaction model Sibyll – past, present and future”. In: *EPJ Web Conf.* 145 (2017). Ed. by B. Pattison, p. 08001. doi: [10.1051/epjconf/201614508001](https://doi.org/10.1051/epjconf/201614508001) (cited on page 13).
- [27] C. Kopper et al. <https://github.com/claudiok/clsim> (cited on page 13).
- [28] D. Chirkin et al. “Photon Propagation using GPUs by the IceCube Neutrino Observatory”. In: *2019 15th International Conference on eScience (eScience)*. 2019, pp. 388–393. doi: [10.1109/eScience.2019.00050](https://doi.org/10.1109/eScience.2019.00050) (cited on page 13).
- [29] J. P. Y. Garza. “Measurement of neutrino oscillations in atmospheric neutrinos with the IceCube DeepCore detector”. PhD thesis. Berlin, Germany: Humboldt-Universität zu Berlin, Mathematisch-Naturwissenschaftliche Fakultät I, 2014. doi: [10.18452/17016](https://doi.org/10.18452/17016) (cited on page 14).
- [30] J. Lundberg et al. “Light tracking for glaciers and oceans: Scattering and absorption in heterogeneous media with Photonics”. In: *Nucl. Instrum. Meth.* A581 (2007), pp. 619–631. doi: [10.1016/j.nima.2007.07.143](https://doi.org/10.1016/j.nima.2007.07.143) (cited on page 14).
- [31] A. Cooper-Sarkar, P. Mertsch, and S. Sarkar. “The high energy neutrino cross-section in the Standard Model and its uncertainty”. In: *JHEP* 08 (2011), p. 042. doi: [10.1007/JHEP08\(2011\)042](https://doi.org/10.1007/JHEP08(2011)042) (cited on page 15).